

Bi-level Off-policy Reinforcement Learning for Volt/VAR Control Involving Continuous and Discrete Devices

Haotian Liu, *Graduate Student Member, IEEE*, Wenchuan Wu, *Fellow, IEEE*

Abstract—In Volt/Var control (VVC) of active distribution networks (ADNs), both slow timescale discrete devices (STDDs) and fast timescale continuous devices (FTCDs) are involved. The STDDs such as on-load tap changers (OLTC) and FTCDs such as distributed generators should be coordinated in time sequence. Such VVC is formulated as a two-timescale optimization problem to jointly optimize FTCDs and STDDs in ADNs. Traditional optimization methods are heavily based on accurate models of the system, but sometimes impractical because of their unaffordable effort on modelling. In this paper, a novel bi-level off-policy reinforcement learning (RL) algorithm is proposed to solve this problem in a model-free manner. A Bi-level Markov decision process (BMDP) is defined to describe the two-timescale VVC problem and separate agents are set up for the slow and fast timescale sub-problems. For the fast timescale sub-problem, we adopt an off-policy RL method soft actor-critic with high sample efficiency. For the slow one, we develop an off-policy multi-discrete soft actor-critic (MDSAC) algorithm to address the curse of dimensionality with various STDDs. To mitigate the non-stationary issue existing in the two agents' learning processes, we propose a multi-timescale off-policy correction (MTOPC) method by adopting importance sampling technique. Comprehensive numerical studies not only demonstrate that the proposed method can achieve stable and satisfactory optimization of both STDDs and FTCDs without any model information, but also support that the proposed method outperforms existing two-timescale VVC methods.

Index Terms—Volt/var control, reinforcement learning, bi-level, multi-timescale, active distribution networks

I. INTRODUCTION

WITH increasing penetration level of distributed generations (DG) [1], modern distribution networks are challenged with severe operating problems such as voltage violations and high network losses. As the common practice, active distribution networks (ADN) have integrated Volt/VAR control (VVC) to optimize the voltage profile and reduce network losses by employing not only the discrete regulation equipments such as on-load tap changers (OLTC) and capacitor banks (CB), but also the continuous control facilities such as the DGs and static var compensators (SVC).

Typically the original VVC task is described as a mixed integer nonlinear programming problem with variables standing for strategies of voltage regulation devices and reactive

power resources. While general symbolic solutions of such problem are hardly available, a variety of methods have been studied and led to various schemes of VVC, which could be categorized via control architectures into the centralized VVC [2], [3], distributed VVC [4], [5], decentralized VVC [6], [7].

Even though the existing VVC methods have achieved considerable performance in traditional distribution networks, most of them rely heavily on the accurate network model. These model-based methods are seriously challenged when an accurate model is expensive or sometimes impractical to maintain in a fast developing ADN with increasing complexity and numerous components [7]–[10]. In the recent years, the research on deep reinforcement learning (DRL) has shown desirable potential on coping with the incomplete model challenges in video game [11]–[13] and multiple areas in power grid operation, including energy trading [14], network reconfiguration [10], frequency control [15], [16] and so on. Hence, many inspiring DRL-based VVC methods has been proposed recently such as [7], [9], [17]–[20]. Such DRL-based VVC methods have empowered the agent in the ADN operating utility to learn a near-optimal strategy by interacting with the actual ADN and mining the optimization process data without an accurate ADN model [21].

Moreover, the characteristics of controlled devices determine the nature of the VVC problem. Two types of devices considered by modern VVC in ADNs are described in table I, including the Slow Timescale Discrete Devices (STDD) and Fast Timescale Continuous Devices (FTCD). As shown in fig. 1, we assume FTCDs take k steps in one STDD step.

TABLE I
TWO TYPES OF DEVICES CONSIDERED BY MODERN VVC IN ADNS

Item	STDD	FTCD
Variable	Discrete	Continuous
Timescale	Slow (in hours)	Fast (in minutes) ^o
Number	Relatively small	Large
Control Price	Limited switching times	Flexible
Devices	OLTCs, CBs, ...	DGs, SVCs,* ...

^o The fast timescale depends heavily on communications.

* The location of SVCs is similar to STDD.

In the active distribution networks with both STDDs and FTCDs, all control devices are supposed to work concurrently and cooperatively, while most of the existing VVC works consider either of them. Because of the huge difference of the natures listed in table I especially the timescale fig. 1, a proper

This work was supported in part by State Grid Corporation of China Project “Research on Coordinated Strategy of Multi-type Controllable Resources Based on Collective Intelligence in an Energy Internet Environment”.

H. Liu and W. Wu (Corresponding Author) are with the State Key Laboratory of Power Systems, Department of Electrical Engineering, Tsinghua University, Beijing 100084, China (email:lht18@mails.tsinghua.edu.cn, wuwench@tsinghua.edu.cn).

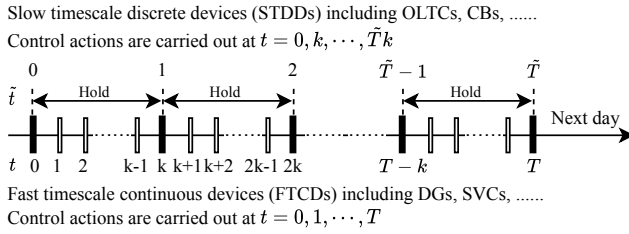


Fig. 1. The timeline of two types of devices in the ADNs.

optimization and control method which fully utilizes the fast speed of FTCDs and the limited STDD actions is non-trivial.

With the assumption of oracle models of ADNs, some researchers have developed optimization-based multi-timescale VVC methods such as [20], [22]–[26]. For example, [24] presents a multi-object coordinated VVC method with the slow timescale as MINLP to optimize the power loss and control actions, and the fast timescale as NLP to minimize the voltage deviation. [24] handles the two stages separately by applying a searching method to solve the MINLP and a scenario-based method to solve the NLP. Instead, [22] formulates the slow timescale VVC as a robust optimization problem and guarantees the worst case in the fast timescale, which may leads to conservativeness or poor convergence. To solve the slow timescale MINLP more efficiently online, [20] has incorporated a DRL algorithm called deep Q network (DQN) to boost the solution, while optimizing the FTCDs with a model-based second-order cone program.

However, to coordinate the FTCDs and STDDs in two timescales and conduct efficient VVC in a model-free manner, it is indispensable for us to develop DRL-based multi-timescale VVC methods. Among the DRL-based VVC methods, most of them target at single-timescale. For example, authors in [9] proposed a safe off-policy RL algorithm to optimize STDDs hourly by formulating the voltage constraints explicitly and considering the device switching cost. In contrast, references [7], [19] are designed to optimize the FTCDs in minutes by incorporating and improving continuous RL algorithms. As for multi-timescale (two-timescale) VVC, reference [20] applied DQN to the slow timescale optimization problem, but depended on oracle model in the fast timescale optimization. Research on DRL-based VVC for both fast and slow timescales, which could achieve model-free optimization, is still urgently needed.

Unfortunately, DRL algorithms for two-timescale agent with such different natures shown in table I are non-trivial and rarely studied. A reasonable solution is to set up RL agents for both timescales individually like fig. 2, so as to satisfy natures of FTCDs and STDDs. However, for the training processes of the agents, traditional RL approaches such as Q-learning are poorly suited. The most fundamental issue is that the policy of the fast timescale agent (FTA) in the lower layer is changing as training processes, and the environment becomes non-stationary from the perspective of slow timescale agent (STA) in the upper layer [27]. In another way, at every decision time of STA, the next step is not only depended on the STDDs' actions of STA itself, but also depended on the subsequent

FTCDs' actions of FTA. This issue extremely challenges the learning stability and prevents the use of experience replay off-policy RL algorithms, which are generally more efficient than the on-policy ones [28]. Besides, the STA involves multiple STDDs and is bothered by the curse of dimensionality in action space.

In this paper, we propose a novel bi-level off-policy RL algorithm and develop a two-timescale VVC accordingly to jointly optimize FTCDs and STDDs in ADNs in a model-free manner. As shown in fig. 2, we first formulate the two-timescale VVC problem in the bi-level RL framework with separate STA and FTA established. Then, the two agents are implemented with detailed designed actor-critic algorithms. Finally, STA and FTA are trained jointly by introducing the multi-timescale off-policy correction technique to eliminate the non-stationary problem. The proposed model-free two-timescale VVC method not only ensures the stability of learning by the coordination of STA and FTA, but also performs off-policy learning with desirable sample efficiency.

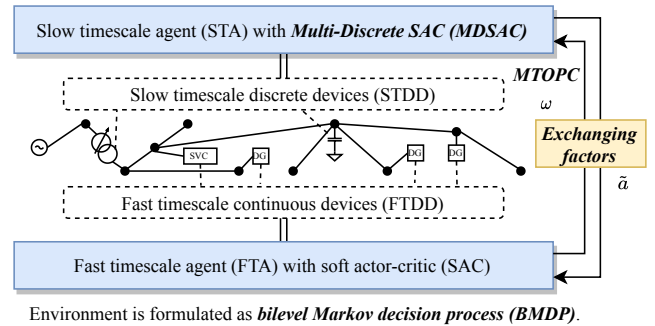


Fig. 2. Overall structure of the proposed bi-level off-policy RL for two-timescale VVC in ADNs. The contributions of this paper are **highlighted**.

Comparing with previous studies on VVC in ADNs, the unique contributions of this paper are summarized as follows.

- 1) To realize model-free optimization of FTCDs and STDDs described table I together, we design a mathematical formulation called bi-level Markov decision process to describe the two-timescale environment. A bi-level off-policy RL framework is proposed accordingly, where two agents FTA and STA are set up for the FTCDs and STDDs respectively and are both trained with off-policy RL algorithms to exploit the samples efficiently.
- 2) To cope with the non-stationary challenge of learning the two agents in two different timescales, our bi-level off-policy RL framework conduct coordination between STA and FTA instead of training them separately. In this context, we propose a technique called multi-timescale off-policy correction (MTOPC). With MTOPC, the bias of STA learning under the disturbance of FTA can be effectively eliminated. Such factors make the application of off-policy RL algorithms available for the STA.
- 3) For the FTAs, the soft actor-critic (SAC) with continuous actions is adapted to learn a stochastic VVC policy; and for the STAs, we develop a multi-discrete soft actor-critic (MDSAC) algorithm to reduce the complexity of training and improve the efficiency. Comparing with

the state-of-art RL algorithms, MDSAC can produce discrete action values for all STDDs simultaneously but alleviating the curse of dimensionality challenge.

The rest of this paper is organized as follows. Section II formulates the two-timescale VVC problem in this paper, and also introduces key concepts and basic methods of RL as preliminaries. Then in section III, the details of the proposed bi-level off-policy RL algorithm are derived and presented, and a two-timescale VVC is developed accordingly. Moreover, in section IV, the results of the numerical study on the proposed two-timescale VVC are shown and analyzed. Finally, section V concludes this paper.

II. PRELIMINARIES

In this section, we firstly formulate the two-timescale VVC problem in this paper. Then, the settings of Markov decision process and its variants used in this paper is introduced. In the last subsection, we cover the preliminaries of reinforcement learning and actor-critic framework to support section III.

A. Two-timescale VVC Problem Formulation

In this paper, we consider an ADN with $n + 1$ nodes. It can be depicted by an undirected graph $\mathcal{G}(\mathcal{N}, \mathcal{E})$ with the collection of all nodes $\mathcal{N} = 0, \dots, n$ and the collection of all branches $\mathcal{E} = (i, j) \in \mathcal{N} \times \mathcal{N}$. The point of common coupling (PCC) is located at node 0 with a substation connected to the power grid simulated by a generation.

Both STDDs and FTCDs are installed in the ADN. STDDs include n_{OLTC} OLTCs and n_{CB} CBs. The tap of i th OLTC is $T_{O,i}$ and the tap of i th CB is $T_{B,i}$. Typically, the number of taps are odd integers $\overline{T_{O,i}}, \overline{T_{B,i}}$. FTCDs include n_{DG} DGs and n_{SVC} SVCs. The reactive power of i th DG is $Q_{G,i}$ and that of i th SVC is $Q_{S,i}$. Without loss of generality, we assume that all STDDs and FTCDs are installed on different nodes in \mathcal{N} .

In a slow-timescale VVC, the taps of OLTCs and CBs are optimized following the objective in eq. (1) [9]. T is the number of slow-timescale VVC steps in one day and t is one of the steps. P_{loss} is the active power loss of the ADN, and $T_{O, \text{loss}}, T_{B, \text{loss}}$ are the acting loss of OLTCs and CBs accordingly. We have $T_{O, \text{loss}}^{(t)} = \sum_{i=1}^{n_{\text{OLTC}}} |T_{O,i}^{(t)} - T_{O,i}^{(t-1)}|$ and $T_{B, \text{loss}}^{(t)} = \sum_{i=1}^{n_{\text{CB}}} |T_{B,i}^{(t)} - T_{B,i}^{(t-1)}|$ when $t > 0$ and $T_{O, \text{loss}}(0) = T_{B, \text{loss}}(0) = 0$. C_P, C_O, C_B are the price coefficients of $P_{\text{loss}}, T_{O, \text{loss}}, T_{B, \text{loss}}$ accordingly. $\underline{V}, \overline{V}$ are the voltage lower and upper limit, and V_i is the voltage at node i .

$$O_S = \min \sum_{\tilde{t}=0}^{\tilde{T}-1} \left[C_P P_{\text{loss}}^{(\tilde{t})} + C_O T_{O, \text{loss}}^{(\tilde{t})} + C_B T_{B, \text{loss}}^{(\tilde{t})} \right] \quad (1)$$

$$s.t. \quad \underline{V} \leq V_i^{(\tilde{t})} \leq \overline{V}, \quad \forall i \in \mathcal{N}, \tilde{t} \in [0, \tilde{T}]$$

As for the fast-timescale VVC, Q_G, Q_S are optimized given the tap settings from the slow timescale. Let T be the number of fast-timescale VVC steps in one day, and t be one of the steps. Then the problem is formulated as eq. (2) [5].

$$O_F = \min \sum_{t=0}^{T-1} \left[C_P P_{\text{loss}}^{(t)} \right] \quad (2)$$

$$s.t. \quad \underline{V} \leq V_i^{(t)} \leq \overline{V}, \quad \forall i \in \mathcal{N}, t \in [0, T]$$

The DGs are typically designed with redundant rated capacity for safety reasons and operate under maximum power point tracking (MPPT) mode. Hence, the controllable range of the reactive power of DGs can be determined by the rated capacity $S_{G,i}$ and maximum power output $\overline{P_{G,i}}$. The reactive power range of controllable devices is $|Q_{G,i}| \leq \sqrt{S_{G,i}^2 - \overline{P_{G,i}}^2}$. Also, we have $\underline{Q_{C,i}} \leq Q_{C,i} \leq \overline{Q_{C,i}}$ where $\underline{Q_{C,i}}, \overline{Q_{C,i}}$ are the bounds of the i th SVC.

Because STDDs and FTCDs both exists in the ADN and need to be coordinated properly, the two problems eqs. (1) and (2) are combined in this paper as eq. (3) assuming that T is a integer multiple of \tilde{T} and $k = T/\tilde{T}$.

$$O_T = \min_{T_O, T_B} \sum_{\tilde{t}=0}^{\tilde{T}-1} \left[C_O T_{O, \text{loss}}^{(k\tilde{t})} + C_B T_{B, \text{loss}}^{(k\tilde{t})} + C_P \min_{Q_G, Q_C} \sum_{\tau=0}^{k-1} P_{\text{loss}}^{(k\tilde{t}+\tau)} \right] \quad (3)$$

$$s.t. \quad \underline{V} \leq V_i^{(k\tilde{t}+\tau)} \leq \overline{V},$$

$$\forall i \in \mathcal{N}, t \in [0, T], \tau \in [0, k]$$

Note that in a model-based optimization method, the VVC problems including eqs. (1) to (3) are solved with power flow constraints. In this paper, we focus on a situation that the accurate power flow model is not available.

B. Markov Decision Process and Reinforcement Learning

A fundamental assumption of reinforcement learning is that the environment can be described as an MDP. The classic definition of an MDP is shown in definition II.1.

Definition II.1 (Markov Decision Process). A Markov decision process is a tuple $(\mathcal{S}, \mathcal{A}, p, r, \rho_0)$, where

- \mathcal{S} is the state space,
- \mathcal{A} is the action space,
- $p : \mathcal{S} \times \mathcal{A} \times \mathcal{S} \rightarrow \mathbb{R}^+ = [0, \infty)$ is the transition probability distribution of the next state $s' \in \mathcal{S}$ at time $t + 1$ with the current state $s \in \mathcal{S}$ and the action $a \in \mathcal{A}$ at time t ,
- $r : \mathcal{S} \times \mathcal{A} \times \mathcal{S} \rightarrow \mathbb{R}$ is the immediate reward received after transiting from state s to s' due to action a ,
- $\rho_0 : \mathcal{S} \rightarrow \mathbb{R}^+$ is the probability distribution of the initial state s_0 .

In the standard continuous control RL setting, an agent interacts with an environment (MDP) over periods of time according to a policy π . The policy can be either deterministic, which means $a = \pi(s)$, or stochastic, which means $a \sim \pi(\cdot|s)$. In this paper, stochastic policies are adapted. From the definition of MDP, we can tell that if the environment is stationary, the cumulative reward can be improved by optimizing π . Classically, the objective of RL at time t is to maximize the expectation of the sum of discounted rewards $G_t = \sum_{i=t+1}^T \gamma^i r(s_i, a_i, s_{i+1})$ where $\gamma \in [0, 1)$ is the discount factor, and T is the length of episode. A well-performing RL algorithm will learn a good policy π from ideally minimal interactions with the environment, as $\max J(\pi) = \mathbb{E}_{\tau \sim \pi} [G(\tau)]$. Here τ is a trajectory of states

and actions noted as $\{s_0, a_0, s_1, a_1, \dots, s_{T-1}, a_{T-1}, s_T\}$ and $G(\tau) = G_0, (s, a) \in \tau, \tau \sim \pi$ is a trajectory with π applied.

To get an optimal policy, one has to evaluate the policy π under unknown environment transition dynamics p and conduct improvement. In reinforcement learning, such evaluation is carried out by defining two value functions $V^\pi(s)$ and $Q^\pi(s, a)$ as shown in eq. (4). $V^\pi(s)$ is the state-value function representing the expected discounted reward after state s with the policy π .

$Q^\pi(s, a)$ is the state-action value function representing the expected discounted reward after taking action a at state s with the policy π .

$$\begin{aligned} V^\pi(s) &= \mathbb{E}_{\tau \sim \pi} \left[\sum_{t=0}^T \gamma^t r_t \mid s_0 = s \right] \\ Q^\pi(s, a) &= \mathbb{E}_{\tau \sim \pi} \left[\sum_{t=0}^T \gamma^t r_t \mid s_0 = s, a_0 = a \right] \\ V^\pi(s) &= \mathbb{E}_{a \sim \pi} Q^\pi(s, a) \end{aligned} \quad (4)$$

According to the Bellman theorem and the Markov feature of MDP, the value functions can be recursively derived as eq. (5),

$$\begin{aligned} V^\pi(s) &= \mathbb{E}_{\substack{a \sim \pi(\cdot|s) \\ s' \sim p(\cdot|s,a)}} [r(s, a, s') + \gamma V^\pi(s')] \\ Q^\pi(s, a) &= \mathbb{E}_{s' \sim p(\cdot|s,a)} \left[r(s, a, s') + \gamma \mathbb{E}_{a' \sim \pi(\cdot|s')} Q^\pi(s', a') \right] \end{aligned} \quad (5)$$

where s' is the next state of s , and a' is the next action. With eq. (5), the value functions can be relaxed from the whole trajectory but updated with batch of transitions.

III. METHODS

In this section, we propose a novel bi-level off-policy reinforcement learning algorithm to solve the two-timescale VVC in ADNs. A summarized version of the RL-based two-timescale VVC is presented in section III-E.

We firstly propose a variant of MDP called bi-level Markov decision process (BMDP) in section III-A to describe the environment in two timescales. The two-timescale VVC problem in section II-A is further formulated into BMDP accordingly.

Then, as shown in figs. 2 and 3, two agents FTA and STA are set up for the two timescales. We adopt the well-known off policy RL algorithm SAC for FTA, which is described in section III-B. To alleviate the curse of dimensionality challenge and improve the efficiency of STA, section III-C propose a novel algorithm MDSAC which allow the STA to decide actions for all STDDs simultaneously with outstanding sample efficiency.

Finally, instead of simply training FTA and STA separately, we calculate the exchanging factors between FTA and STA by our innovated MTOPC technique in section III-D. It allows the FTA and STA trained together to optimize BMDP in a stationary manner based on the inherent Markov property of BMDP.

A. Two-timescale VVC in Bi-level Markov Decision Process

The standard RL setting in section II-B considers only a single timescale, which does not match the two-timescale VVC problem in section II-A. Hence, BMDP is defined as a variant of MDP in definition III.1 to describe the environment (two-timescale VVC problem). The transition probability p is still unknown to the agents. Note that though similar settings exist in some previous works related to hierarchical RL such as [29], BMDP is specially reformed for the two-timescale setting.

Definition III.1 (Bi-level Markov Decision Process). A bi-level Markov decision process is a joint of two MDPs defined in definition II.1 in two timescales, and is defined as a tuple $(k, \mathcal{S}, \mathcal{A}_s, \mathcal{A}_f, r_s, r_l, p, \rho_0)$. Most of the symbols follow definition II.1, and $\mathcal{A} = \mathcal{A}_s \cup \mathcal{A}_f$. The incremental parts are described as follows.

- \mathcal{A}_s is the slow action space,
- \mathcal{A}_f is the fast action space,
- k is the timescale ratio and the \mathcal{A}_s is only available every k steps of the \mathcal{A}_f ,
- when $t \bmod k \neq 0$, the fast action $a \in \mathcal{A}_f$ makes that $s' \sim p(\cdot|s, a)$,
- when $t \bmod k = 0$, two transitions happens consequently: 1) the slow action $\tilde{a} \in \mathcal{A}_s$ is applied and the state transits from \tilde{s} to s as $s \sim p(\cdot|\tilde{s}, \tilde{a})$; 2) the fast action $a \in \mathcal{A}_f$ is applied and $s' \sim p(\cdot|s, a)$,
- $r_s : \mathcal{S} \times \mathcal{A}_s \times \mathcal{S} \rightarrow \mathbb{R}$ is the immediate reward received in slow timescale after transiting from state \tilde{s} to \tilde{s}' due to action \tilde{a} ,
- $r_f : \mathcal{S} \times \mathcal{A}_f \times \mathcal{S} \rightarrow \mathbb{R}$ is the immediate reward received in fast timescale after transiting from state s to s' due to action a .

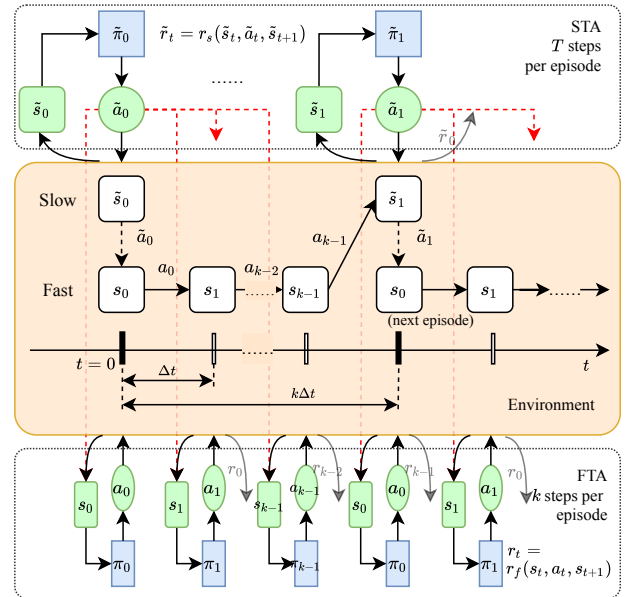


Fig. 3. The setting of BMDP and the agents STA, FTA in this paper.

Orange painted part in fig. 3 illustrates BMDP step by step. The setting of BMDP has ensured the environment is Markovian from the perspective of bi-level. In each episode (k

steps) of the fast layer, the initial state depends on the certain slow action. We therefore has to include the corresponding slow action in the state explicitly, which is emphasized by red dashed lines. The slow actions $\tilde{a}_0, \tilde{a}_1, \dots$ can be seen as the exchanging factors from STA to FTA as shown in fig. 2.

Obviously, the transition from \tilde{s}_0 to \tilde{s}_1 depends not only on the slow action \tilde{a}_0 , but also on the k fast actions a_0, a_1, \dots, a_{k-1} . Hence, in the view of slow level, the environment does not satisfy Markov property. In another way, **BMDP is Markovian bi-levelly in fast level, but non-Markovian in slow level**. In the following section III, one of the major ideas is to take full advantage of the inherent Markov property of BMDP and carry out stable learning and control process in both timescales.

To formulate the two-timescale VVC problem eq. (3) into BMDP, the specific definitions of episodes, state spaces, action spaces and reward functions are designed as follows.

1) *Episode*: An episode of STA is defined as one day, and the step size Δt is one hour. We have $\tilde{T} = 24$ total steps in one episode. An episode of FTA includes $k = 12$ steps in one STA step with $\Delta \hat{t} = 5\text{min}$. Note that $T, k, \Delta t, \Delta \hat{t}$ are all alterable while satisfying $\Delta t = k\Delta \hat{t}$.

2) *State Space*: The common state of BMDP is defined as a vector $(\mathbf{P}, \mathbf{Q}, \mathbf{V}, \mathbf{T}_O, \mathbf{T}_B, t)$, where \mathbf{P}, \mathbf{Q} are the vectors of nodal active/reactive power injections $P_i, Q_i (\forall i \in \mathcal{N})$, \mathbf{V} is the vector of voltage magnitudes $V_i (\forall i \in \mathcal{N})$, $\mathbf{T}_O = [T_{O,1}, \dots, T_{O, n_{\text{OLTC}}}]^T$ is the vector of OLTC taps, $\mathbf{T}_B = [T_{B,1}, \dots, T_{B, n_{\text{CB}}}]^T$ is the vector of CB taps, t is the time in one day.

3) *Action Spaces*: For FTA, the action space \mathcal{A}_f includes all the controllable reactive power of FTCDs, that is, $[Q_{G,1}, \dots, Q_{G, n_{\text{DG}}}, Q_{C,1}, \dots, Q_{C, n_{\text{SVC}}}]^T$. Since the reactive power generations are continuous in section II-A, \mathcal{A}_f is defined as a box space with the lower bound $[-Q_{G,1}, \dots, -Q_{G, n_{\text{DG}}}, Q_{C,1}, \dots, Q_{C, n_{\text{SVC}}}]$, and upper bound $[\overline{Q_{G,1}}, \dots, \overline{Q_{G, n_{\text{DG}}}}, \overline{Q_{C,1}}, \dots, \overline{Q_{C, n_{\text{SVC}}}}]$, where $\overline{Q_{G,i}} = \sqrt{S_{G,i}^2 - P_{G,i}^2}$.

For STA, the action space \mathcal{A}_s includes all the tap settings of STDDs, that is, $(\mathbf{T}_O, \mathbf{T}_B)$. Each tap setting $T_{O,i}$ or $T_{B,i}$ can be selected from $\overline{T_{O,i}}$ or $\overline{T_{B,i}}$ taps, so \mathcal{A}_s is a discrete space with multi dimensions, also known as multi-discrete space. The dimensions are listed in the vector $[\overline{T_{O,1}}, \dots, \overline{T_{O, n_{\text{OLTC}}}}, \overline{T_{B,1}}, \dots, \overline{T_{B, n_{\text{CB}}}}]^T$.

4) *Reward Functions*: The reward functions maps a certain transition to a single value to cumulate and maximize.

For the fast timescale, note a transition as (s, a, s') where $s, s' \in \mathcal{S}$ and $a \in \mathcal{A}_f$. Then r_f is defined as eq. (6) according to the inner minimization of eq. (3). Here $[\cdot]_+$ is the rectified linear unit function defined as $[x]_+ = \max(0, x)$, C_V is a penalty multiplier for the voltage constraints, and V_{loss} is a smooth index of the voltage violations called voltage violation

rate (VVR).

$$r_f(s, a, s') = -C_P P_{\text{loss}}(s') - C_V V_{\text{loss}}(s') \quad (6)$$

$$P_{\text{loss}}(s') = \sum_{i \in \mathcal{N}} P_i(s'), \quad (7)$$

$$V_{\text{loss}}(s') = \sqrt{\sum_{i \in \mathcal{N}} [(V_i(s') - \bar{V})_+^2 + [V - V_i(s')]_+^2]} \quad (8)$$

For the slow timescale, the transition is noted as $(\tilde{s}, \tilde{a}, \tilde{s}')$, where $\tilde{s}, \tilde{s}' \in \mathcal{S}$ and $\tilde{a} \in \mathcal{A}_s$. Also, as shown in fig. 3, we have as series of fast timescale samples between \tilde{s} and \tilde{s}' . Note them as $s_0, a_0, s_1, a_1, \dots, s_{k-1}, a_{k-1}, s_k$ where $s_k = \tilde{s}'$. Since the objective of the STA considers switching cost of STDDs, the reward function of the slow timescale r_s includes the switching cost part and the cumulative reward of the fast timescale.

$$r_s(\tilde{s}, \tilde{a}, \tilde{s}', \{s_\tau, a_\tau | \tau \in [0, k]\}, s_k) = -C_O T_{O, \text{loss}}(\tilde{s}, \tilde{s}') - C_B T_{B, \text{loss}}(\tilde{s}, \tilde{s}') - R_f(\{s_\tau, a_\tau | \tau \in [0, k]\}, s_k) \quad (9)$$

$$T_{O, \text{loss}}(\tilde{s}, \tilde{s}') = \sum_{i=1}^{n_{\text{OLTC}}} |T_{O,i}(\tilde{s}') - T_{O,i}(\tilde{s})| \quad (10)$$

$$T_{B, \text{loss}}(\tilde{s}, \tilde{s}') = \sum_{i=1}^{n_{\text{CB}}} |T_{B,i}(\tilde{s}') - T_{B,i}(\tilde{s})| \quad (11)$$

$$R_f(\{s_\tau, a_\tau | \tau \in [0, k]\}, s_k) = \sum_{\tau=0}^{k-1} r_f(s_\tau, a_\tau, s_{\tau+1}) \quad (12)$$

To solve BMDP, two agents STA and FTA are set up for the slow and fast timescales respectively, as shown in fig. 3. The policy of STA is marked as $\tilde{\pi}$, while that of FTA is π . An intuitive method would be training STA and FTA separately. However due to the fact that the environment is non-Markovian from the view of STA, it violates the basic assumption of RL algorithms and leads to non-stationary learning process. In section III-D, MTOPC is proposed addressing this challenge.

B. Soft Actor-Critic for FTA

SAC [30] is a state-of-art off-policy RL method for MDPs with continuous action space. It is implemented in the actor-critic framework, where the actor is the stochastic policy $\pi(\cdot|s)$, and the critic is the state-action value function $Q^\pi(s, a)$. π and Q^π are both approximated by deep neural networks (DNN) with parameters noted as ϕ_f and θ_f in practice.

In SAC, the definition of state-action value function is entropy-regularized as

$$Q_f^\pi(s, a) = \mathbb{E}_{\tau \sim \pi} \left[\sum_{t=0}^T \gamma^t r_t + \alpha_f \sum_{t=1}^T \gamma^t H(\pi(\cdot|s_t)) | s_0 = s, a_0 = a \right] \quad (13)$$

where $H(\pi(\cdot|s_t)) = \mathbb{E}_{a \sim \pi(\cdot|s_t)} [-\log \pi(a|s_t)]$ is the entropy for the stochastic policy at s_t , α_f is the temperature parameter.

During the learning process, all the samples of MDP are stored in the replay buffer \mathcal{D} as $(s, a, r_f, s') \in \mathcal{D}$. To approximate Q_f^π iteratively, Bellman equation is applied to the

entropy-regularized Q_f^π as eq. (14) since $\mathbb{E}_{s',a'} H(\pi(\cdot|s')) = -\mathbb{E}_{s',a'} \log \pi(\cdot|s')$.

$$\begin{aligned} Q_f^\pi(s, a) &\approx \mathbb{E}_{\substack{s' \sim p(\cdot|s, a) \\ a' \sim \pi(\cdot|s')}} \left[r_f + \gamma (Q_f^\pi(s', a') + \alpha_f H(\pi(\cdot|s'))) \right] \\ &= \mathbb{E}_{\substack{s' \sim p(\cdot|s, a) \\ a' \sim \pi(\cdot|s')}} \left[r_f + \gamma (Q_f^\pi(s', a') - \alpha_f \log \pi(a'|s')) \right] \end{aligned} \quad (14)$$

Then, mean-squared Bellman error (MSBE) eq. (15) is minimized to update the Q network. Note $y = r_f + \gamma (Q_f^\pi(s', a') - \alpha_f \log \pi(a'|s'))$. All expectations are approximated with Monte Carlo method.

$$L_f^Q(\phi_f) = \mathbb{E}_{(s, a, r_f, s') \in \mathcal{D}} [Q_{\phi_f} - y]^2 \quad (15)$$

The policy is optimized to maximize the state value function $V^\pi(s) = \mathbb{E}_{a \sim \pi} Q^\pi(s, a)$. In SAC, the reparameterization trick using a squashed Gaussian policy is introduced: $a'_{\theta_f}(s, \xi) = \tanh(\mu_{\theta_f}(s) + \sigma_{\theta_f}(s) \odot \xi)$, $\xi \sim \mathcal{N}(0, \mathbf{I})$, where $\mu_{\theta_f}, \sigma_{\theta_f}$ are two DNNs. Hence, and the policy can be optimized by minimizing eq. (16), where $a' = a'_{\theta_f}(s, \xi)$.

$$L_f^\pi(\theta_f) = - \mathbb{E}_{\substack{\tilde{s} \sim \mathcal{D} \\ \xi \sim \mathcal{N}}} [Q^\pi(s, a') - \alpha_f \log \pi_{\theta_f}(a'|s)] \quad (16)$$

Other practical techniques in [30] are omitted here due to limited space.

C. Multi-Discrete Soft Actor-Critic for STA

Comparing with the FTA with continuous actions, STA has discrete actions in multi dimensions. It makes fundamental differences in the RL algorithm. Therefore, we propose a variant of SAC called multi-discrete soft actor-critic (MDSAC) as follows. MDSAC fully suits the multi-discrete action space of STA and can carry out high efficiency training in an off-policy manner.

1) *Policy DNN Architecture*: Because the policy should select an action for each of the STDDs, we design a multi-head DNN for $\tilde{\pi}$. Note $n_s = n_{CB} + n_{OLTC}$ as the number of STDDs, and m_i as the number of taps of i th STDD. As shown in fig. 4a, \tilde{s} is mapped to a shared representation, which are passed to n_s heads with hidden layers. The i th head produces m_i digits, passes them to the softmax layer, and receives a vector of m_i digits $\tilde{\pi}^i(\tilde{s}) = [\tilde{\pi}^i(\tilde{a}_1^i, \tilde{s}), \dots, \tilde{\pi}^i(\tilde{a}_{m_i}^i, \tilde{s})]^T$, where $\tilde{a}_1^i, \dots, \tilde{a}_{m_i}^i$ are all the possible actions of i th STDD. Note that $\sum_{j=1}^{m_i} \tilde{\pi}_j^i(\tilde{s}) = 1$. Finally, the probability value of a certain action \tilde{a} is $\tilde{\pi}(\tilde{a}|\tilde{s}) = \prod_{i=1}^{n_s} \tilde{\pi}^i(\tilde{a}^i, \tilde{s})$.

2) *Value DNN Architecture*: One of the most challenging problem in off-policy RL with multi-discrete action space is that the state-action value function is non-trivial to implement. Classically, if the action space is discrete, the state-action value function is designed as $Q: \mathcal{S} \rightarrow \mathbb{R}^m$, where m is the number of actions. However, with multiple devices, it upgrades to $Q_s: \mathcal{S} \rightarrow \mathbb{R}^{m_1} \times \mathbb{R}^{m_2} \dots \times \mathbb{R}^{m_{n_s}}$ mathematically. It means that Q_s has $\prod_{i=1}^{n_s} m_i$ outputs. When n_s increases, the cost of memory and CPU time will grow exponentially. Worse still is that bloated Q_s outputs requires much more samples to train,

which is unaffordable in ADNs. Such exponential complexity can be seen as the curse of dimensionality problem and hinders the implementation of STA in practice.

To alleviate the problem above, we introduce a device decomposition technique to the value DNN architecture inspired by [31], where the value function is relaxed as the sum of independent value functions with local states and actions of each agent in multi-agent settings. A limitation of [31] is that such sum combination may reduce the approximation performance of the DNN. In MDSAC, we introduce \tilde{s} -adaptive affine parameters $c(\tilde{s})$ to address the limitation.

As shown in fig. 4b, the share representation is fed to two parts: 1) the i th head produces a vector $Q_s^i(\tilde{s})$ of m_i scalars noted as $Q_s^i(\tilde{s}, \tilde{a}_j^i), j \in [1, m_i]$; 2) a vector $c(\tilde{s})$ containing $n_s + 1$ scalars, where $c(\tilde{s}) = [c_0, c_1, \dots, c_{n_s}]^T$. For a certain action \tilde{a} , the device-wise state-action values are selected as $Q_s^1(\tilde{s}, \tilde{a}^1), \dots, Q_s^{n_s}(\tilde{s}, \tilde{a}^{n_s})$. Then, they are combined in an affine mixing network with ratios $c(\tilde{s})$, as eq. (17). Because the ratios $c(\tilde{s})$ are also generate from DNNs, the flexibility of approximation to actual Q_s is generally boosted comparing with [31]. Also, $c_0(\tilde{s})$ learns a base value for each state, which is inherently similar to the well-known dueling network architecture [32].

$$Q_s(\tilde{s}, \tilde{a}) = c_0(\tilde{s}) + \sum_{i=1}^{n_s} c_i(\tilde{s}) Q_s^i(\tilde{s}, \tilde{a}^i) \quad (17)$$

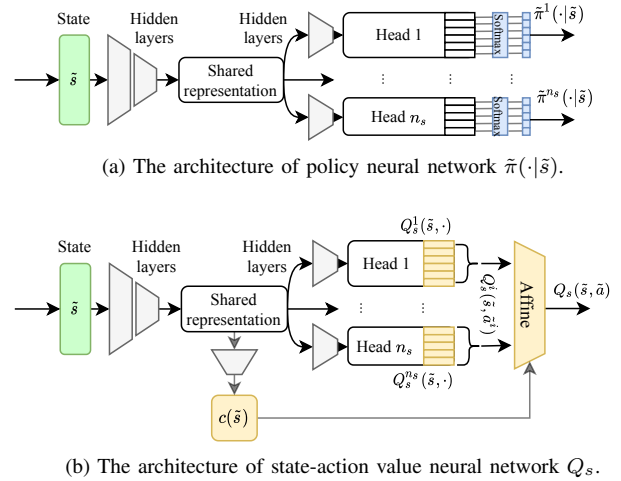


Fig. 4. DNN architecture design of $\tilde{\pi}$ and Q_s .

3) *Updates of Actor and Critic*: Since the action space is discrete, the policy maps \tilde{s} to the probability value of action \tilde{a} instead of a probability density function. As a result, the expectation on the policy ($\mathbb{E}_{\tilde{a}' \sim \tilde{\pi}(\cdot|\tilde{s}')}$) can be calculated explicitly instead of in a Monte Carlo way. That means the state value function can be expressed as

$$\begin{aligned} V_s^{\tilde{\pi}}(\tilde{s}) &= \mathbb{E}_{\tilde{a} \sim \tilde{\pi}(\cdot|\tilde{s})} [Q_s(\tilde{s}, \tilde{a}) - \alpha_s \log \tilde{\pi}(\tilde{a}|\tilde{s})] \quad (18) \\ &= \sum_{i=1}^{n_s} \tilde{\pi}^i(\tilde{s})^T [c_i(\tilde{s}) Q_s^i(\tilde{s}) - \alpha_s \log \tilde{\pi}^i(\tilde{s})] + c_0(\tilde{s}) \end{aligned} \quad (19)$$

where the linearity of expectation operator and the mixing network are leveraged.

From eqs. (4) and (5), we have

$$Q_s^{\tilde{\pi}}(\tilde{s}, \tilde{a}) = \mathbb{E}_{\tilde{s}' \sim \tilde{p}(\cdot|\tilde{s}, \tilde{a})} [r_s(\tilde{s}, \tilde{a}, \tilde{s}') + \gamma V_s^{\tilde{\pi}}(\tilde{s}')] \quad (20)$$

where $\tilde{p}(\cdot|\tilde{s}, \tilde{a})$ is the current environment transition probability distribution. Note $\tilde{y}(\tilde{s}'|\tilde{s}, \tilde{a}) = r_s(\tilde{s}, \tilde{a}, \tilde{s}') + \gamma V_s^{\tilde{\pi}}(\tilde{s}')$. If $\tilde{p}(\cdot|\tilde{s}, \tilde{a})$ holds, the expectation can be calculated by Monte Carlo method on \mathcal{D} . However, $\tilde{p}(\cdot|\tilde{s}, \tilde{a})$ is changing with π of FTA varying in section III-B. This is ignored temporarily here and will be corrected in section III-D.

$$L_s^Q(\phi_s) = \mathbb{E}_{(\tilde{s}, \tilde{a}, \tilde{s}', r_s) \sim \mathcal{D}} [\tilde{y}(\tilde{s}'|\tilde{s}, \tilde{a}) - Q_{\phi_s}(\tilde{s}, \tilde{a})]^2 \quad (21)$$

$$L_s^{\pi}(\theta_s) = - \mathbb{E}_{S \sim \mathcal{D}} [V_s^{\tilde{\pi}}(\tilde{s})] \quad (22)$$

Accordingly, the parameters ϕ_s of Q_s and θ_s of $\tilde{\pi}$ can be optimized by minimizing eqs. (21) and (22).

D. Multi-timescale Off-policy Correction

As an off-policy RL algorithm, MDSAC stores all transitions in the experience replay buffer \mathcal{D} . In eq. (20), if $\tilde{p}(\cdot|\tilde{s}, \tilde{a})$ holds as assumed by MDP, the expectation can be calculated with Monte Carlo method by sampling \mathcal{D} , like SAC in section III-B does. However, in BMDP only $p(\cdot|s, a)$ is assumed to be stationary. Mathematically, as shown in fig. 3, the current probability of transition from \tilde{s}_0 to \tilde{s}_1 is

$$\tilde{p}(\tilde{s}_1|\tilde{s}_0, \tilde{a}_0) = p(s_0|\tilde{s}_0, \tilde{a}_0) \prod_{i=0}^{k-1} \pi_i(a_i|s_i) p(s_{i+1}|s_i, a_i) \quad (23)$$

where $s_k = \tilde{s}_1$. While the FTA is training with eq. (16), π is varying from time to time. Hence, we have marked π_0, \dots, π_{k-1} for each FTA step. Though STA needs to calculate the expectation on eq. (23), the data in \mathcal{D} is sampled from another probability distribution,

$$\tilde{p}^0(\tilde{s}_1|\tilde{s}_0, \tilde{a}_0) = p(s_0|\tilde{s}_0, \tilde{a}_0) \prod_{i=0}^{k-1} \pi_i^0(a_i|s_i) p(s_{i+1}|s_i, a_i) \quad (24)$$

where π^0 is the behavior policy used in past, and π^0 is different from the current policy π . Obviously, the samples from \mathcal{D} are not valid for direct Monte Carlo any more. In another way, during the learning process, the past experience of STA is no longer correct for the current learning and can lead to significant bias.

To reuse the samples in \mathcal{D} and leverage the off-policy MDSAC's high sample efficiency, we propose multi-timescale off-policy correction (MTOPC) based on importance sampling (IS) method. IS is widely used in policy gradient RL algorithms like A2C [33] and PPO [34].

To estimate the expectation in eq. (20), MTOPC is derived as eq. (25),

$$\begin{aligned} \mathbb{E}_{\tilde{p}(\cdot|\tilde{s}, \tilde{a})} \tilde{y}(\tilde{s}'|\tilde{s}, \tilde{a}) &= \mathbb{E}_{\tilde{p}^0(\cdot|\tilde{s}, \tilde{a})} \frac{\tilde{p}(\tilde{s}'|\tilde{s}, \tilde{a})}{\tilde{p}^0(\tilde{s}'|\tilde{s}, \tilde{a})} \tilde{y}(\tilde{s}'|\tilde{s}, \tilde{a}) \\ &= \mathbb{E}_{\tilde{p}^0(\cdot|\tilde{s}, \tilde{a})} \frac{p(s_0|\tilde{s}, \tilde{a}) \prod_{i=0}^{k-1} [\pi(a_i|s_i) p(s_{i+1}|s_i, a_i)]}{p(s_0|\tilde{s}, \tilde{a}) \prod_{i=0}^{k-1} [\pi_i^0(a_i|s_i) p(s_{i+1}|s_i, a_i)]} \tilde{y}(\tilde{s}'|\tilde{s}, \tilde{a}) \\ &= \mathbb{E}_{\tilde{p}^0(\cdot|\tilde{s}, \tilde{a})} \prod_{i=0}^{k-1} \frac{\pi(a_i|s_i)}{\pi_i^0(a_i|s_i)} \tilde{y}(\tilde{s}'|\tilde{s}, \tilde{a}) \\ &= \mathbb{E}_{\tilde{p}^0(\cdot|\tilde{s}, \tilde{a})} \omega \cdot \tilde{y}(\tilde{s}'|\tilde{s}, \tilde{a}) = \mathbb{E}_{\mathcal{D}} \omega \cdot \tilde{y}(\tilde{s}'|\tilde{s}, \tilde{a}) \end{aligned} \quad (25)$$

where π is the current FTA policy, π^0 is the behavior (original) policies, and ω is the correction factor calculated by FTA,

$$\omega = \prod_{i=0}^{k-1} \frac{\pi(a_i|s_i)}{\pi_i^0(a_i|s_i)}. \quad (26)$$

Similar technique was also studied by [11] in hierarchical RL instead of the multi-timescale settings.

In practice, $\pi_0(a|s)$ is stored with the transition in \mathcal{D} , and $\pi(a|s)$ is calculated using the latest FTA policy. Because the cumulative product in eq. (26) may lead to high variance and numerical problem, we clip ω as $\omega' = \max(\min(\omega, \bar{\omega}), \underline{\omega})$, where $\underline{\omega}, \bar{\omega}$ are the lower and upper bound for ω' .

Accordingly, eq. (21) is corrected as

$$L_s^Q(\phi_s) = \mathbb{E}_{\mathcal{D}} [\omega' \cdot \tilde{y}(\tilde{s}'|\tilde{s}, \tilde{a}) - Q_{\phi_s}(\tilde{s}, \tilde{a})]^2 \quad (27)$$

with batches of $(\tilde{s}, \tilde{a}, s_0, a_0, \dots, s_{k-1}, a_{k-1}, \tilde{s}', r_s)$ sampled from \mathcal{D} and the latest π .

E. Two-timescale VVC with Bi-level RL

The overall algorithm combining sections III-A to III-D are summarized in algorithm 1. Note that the gradient steps of STA or FTA are carried out in parallel with the controlling process. Typically, one gradient step is executed every one or several control steps.

In real world application, the FTA and STA can be pre-trained with an approximated model directly or with [17].

IV. NUMERICAL STUDY

With distribution test feeders, numerical studies are conducted to validate the advantage of the proposed two-timescale VVC based on bi-level off-policy RL. The two-timescale VVC problem formulated in BMDP is implemented under the scheme of Gym toolkit [35]. A modified version of 33-bus distribution test feeder [36] is simulated as the target ADN. In the 33-bus system, 4 DGs are connected to node 18,22,25,33 with 0.85 MVA rating, 1 OLTC is installed on the branch from node 1 to node 2, and 1 CB is installed on node 8. The OLTC have 11 taps, and the ratio ranges evenly from 0.9 to 1.1. Also, the CB have 11 taps and the output ranges from -1 MVar to 1 MVar evenly. The profile of DGs and loads from a pilot project in eastern China is scaled to [0, 2] and allocated to the existing nodes in the standard case by multiplication. All DGs are assumed to be installed with smart inverters following

Algorithm 1: Two-timescale VVC with Bi-level RL

Given learning rates σ_s, σ_f , temperature parameters α_s, α_f ;
Initialize STA and FTA's policy and value functions'
parameter vectors $\phi_s, \theta_s, \phi_f, \theta_f$;
 $\mathcal{D} \leftarrow \emptyset$;
foreach STA episode **do**
 Get the initial state $\tilde{s}_0, t \leftarrow 0$;
 foreach STA step **do in parallel**
 $\tilde{a}_t \sim \tilde{\pi}(\cdot|\tilde{s}_t)$;
 Feed \tilde{a}_t to the environment, get next state s_0 ;
 $\mathcal{D}_t \leftarrow \emptyset, i \leftarrow 0$;
 foreach FTA step in a k -step episode **do**
 $a_i \sim \pi(\cdot|s_i), p_i \leftarrow \pi(a_i|s_i)$;
 Feed a_i to the environment, get reward $r_{f,i}$,
 next state s_{i+1} ;
 $\mathcal{D}_t \leftarrow \mathcal{D}_t \cup \{(s_i, a_i, r_{f,i}, s_{i+1}, p_i)\}$;
 $i \leftarrow i + 1$;
 end
 Get reward $r_{s,t}$, state $\tilde{s}' \leftarrow s_k$;
 $\mathcal{D} \leftarrow \mathcal{D} \cup \{(\tilde{s}_t, \tilde{a}_t, r_{s,t}, \tilde{s}_{t+1}, \mathcal{D}_t)\}$;
 $t \leftarrow t + 1$;
 end
 foreach FTA gradient step **do in parallel**
 Sample a batch of (s, a, r_f, s') from \mathcal{D} ;
 Update Q_{ϕ_f} with eq. (15):
 $\phi_f \leftarrow \phi_f - \sigma_f \nabla_{\phi_f} L_f^Q(\phi_f)$;
 Update π_{θ_f} with eq. (16):
 $\theta_f \leftarrow \theta_f - \sigma_f \nabla_{\theta_f} L_f^\pi(\theta_f)$;
 end
 foreach STA gradient step **do in parallel**
 Sample a batch of $(\tilde{s}, \tilde{a}, r_s, \tilde{s}', D)$ from \mathcal{D} ;
 Calculate ω with eq. (26);
 Update Q_{ϕ_s} with eq. (27):
 $\phi_s \leftarrow \phi_s - \sigma_s \nabla_{\phi_s} L_s^Q(\phi_s)$;
 Update π_{θ_s} with eq. (22):
 $\theta_s \leftarrow \theta_s - \sigma_s \nabla_{\theta_s} L_s^\pi(\theta_s)$;
 end
end

IEEE 1547. The voltage limitations are set to be $[0.95, 1.05]$. If the power flow does not converge or there is any $V_i > 1.15$ or $V_i < 0.85$ at certain time step, there is thought to be a grid failure and the episode is terminated with a negative reward $r_f = -500$. As suggested in [9], the electricity price C_P is assumed to be \$40/MWh, and the action price C_O and C_B are assumed to be \$0.1/tap. The price of voltage violation rate is set to be \$100/p.u. · 5mins.

A. Proposed and Baseline Algorithms Setup

To compare with traditional two-timescale VVC, we implement an optimization-based benchmark as single-step mixed-integer conic programming (MICP) for STA and second order conic programming (SOCP) for FTA, which is equivalent to the method in [25]. Note that because the actual model is unknown to the operator, optimization methods are carried out

with an approximated model. In this paper, this benchmark is marked as ‘‘A-OPT’’. The one with oracle model is marked as ‘‘OPT’’. But since the optimization is single step-wise, global optimality is not guaranteed.

Since works are still limited regarding DRL-based two-timescale VVC, we implement the method in [20] as the second benchmark called ‘‘S-DQN’’. It adopts the classic DQN algorithm for STA by enumerating all possible STDDs combinations in the Q network and has $\prod_{i=1}^{n_s} m_i$ actions. For FTA, it adopts the SOCP method based on detailed ADN models. Note that when we adopts the approximated model for SOCP, the STA cannot converge to a reasonable range in limited time (100k steps). Hence, we implement S-DQN with oracle models, which is not required by our proposed method.

To show the effectiveness of the proposed MTOPC method, we add the third benchmark called ‘‘Non-OPC’’. This benchmark is the same as the proposed one except for $\omega = 1$ instead of eq. (26).

In the following numerical studies, the proposed method in algorithm 1 is marked as ‘‘Proposed’’. The discrete variables $\mathbf{T}_O, \mathbf{T}_B$ in the state are encoded with one-hot embedding. That is, a certain tap like $T_{o,i}$ is transformed to a $\bar{T}_{o,i}$ -length binary vector $[0, \dots, 1, \dots, 0]^T$ with zeros except for 1 at $T_{o,i}$ -th position. The bound of MTOPC ω is set as $\omega = 0.1, \bar{\omega} = 10$. All DRL-based methods implemented are trained under PyTorch with the parameters of DNNs randomly initialized and updated in batches. The batch size is chosen as 128 and the replay buffer is designed to be a queue with size of $2000 \times 12 = 24000$ FTA steps. All the optimization methods are implemented with Casadi [37] in Python.

B. Optimality and Sample Efficiency

During the experiment, it is observed that 90 episodes are enough for the benchmarks and proposed method to get reasonable solutions. The training process, which is supposed to evaluate on a real system in practice, is simulated and visualized in fig. 5. Since DRL-based algorithms are stochastic methods, experiments are carried out with 3 independent random seeds, and the mean values and error bounds of performances are represented as solid curves and light-colored regions.

Comparing the proposed method with S-DQN, fig. 5 illustrates that the proposed method achieves near-optimal performance on rewards with significantly fewer samples, even without any ADN topology or parameters information. On the other hand, it is observed that S-DQN is better regarding active power loss from the very beginning. This is because S-DQN takes advantage of oracle ADN models, which are not required by the proposed method, for FTA and achieves optimal reactive power distribution of DGs in every step. But for the STA, the efficiency and stability of DQN is surpassed by the proposed MDSAC.

Comparing with A-OPT, the proposed method has avoided the misleading of errors in models as shown in table II. Since the proposed method is data-driven and model-free, its performance may differ from the optimization-based one with oracle model. The major advantage of our proposed method is

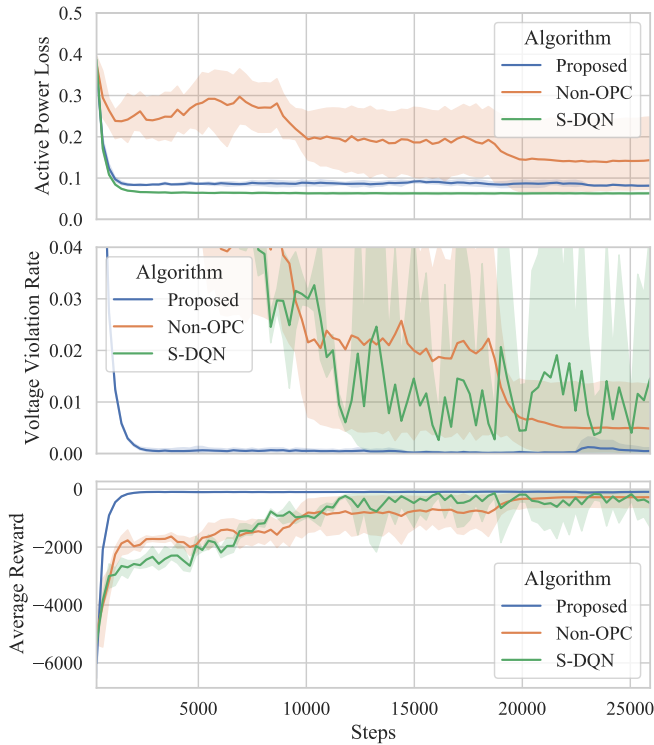


Fig. 5. The training curve of DRL-based methods on the modified 33-bus ADN test feeder.

to learn continuously online, coordinate two-timescale devices together and achieve near-optimal performance in a model-free manner.

TABLE II
QUANTIFIED INDICES OF THE TRAINED AGENT AND BENCHMARKS IN FINAL EPISODE

Algorithm	$P_{\text{loss}}/\text{MW}$	VVR/p.u.	$T_{\text{loss}}/\text{taps}$
	33-bus	33-bus	33-bus
Proposed	8.30e-02	0	2.4
S-DQN	6.05e-02	5.83e-02	4.3
A-OPT	1.08e-01	1.98e-01	7.0
OPT	4.59e-02	0	3.0

C. Effectiveness of MTOPC

As shown in fig. 5, our proposed method with MTOPC achieves near-optimal level of performance in the first 2000 steps, while the “Non-OPC” one without MTOPC needs much more samples and shows higher variance with different random seeds. With certain seeds Non-OPC still learns satisfactory policies after iterations, but with other seeds it doesn’t. The reason is that the expectation itself we have corrected by MTOPC in eq. (25) is a random variable. Even though the estimation is biased, the STA still learns in some cases. Nevertheless, with MTOPC the bias can be eliminated and it improves the stability of the training process.

To explain the effectiveness of MTOPC further, fig. 6 the mean and standard deviation of MTOPC’s ω' in a batch with the proposed method. Similarly, the solid curves stand for

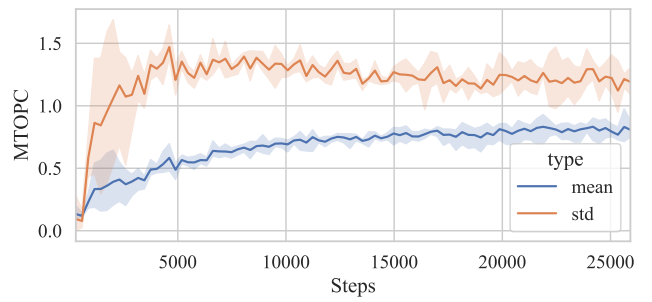


Fig. 6. The mean and standard deviation of MTOPC’s ω' on the modified 33-bus ADN test feeder with the proposed method.

mean value and light-colored regions stand for error bounds across random seeds. In the starting periods, the mean ω' is near the lower bound because the policy of FTA is learning from the scratch. But the deviation of ω' is at a relatively high level, which means the correction is carried out by reducing some samples and increasing the others. While the FTA growing mature, the mean of ω' grows near 1 since the old samples still exist in \mathcal{D} . Also, it is worth mentioning that MTOPC not only benefits STA but also FTA because if the STA finds an optimal policy soon enough, FTA can save the effort of learning on the states with bad STA actions.

V. CONCLUSION

A bi-level off-policy DRL algorithm is proposed for two-timescale VVC with both FTCDs and STDDs coordinated without oracle network topology or parameters. BMDP is defined to formulate the two-timescale VVC problem, and separate agents STA and FTA are implemented with off-policy DRL methods. For STA, a high efficient off-policy algorithm MDSAC is proposed with value decomposition to address the curse of dimensionality. For the coordination between STA and FTA, a novel MTOPC method is proposed to eliminate the inherent disturbance between the two agents. Numerical studies conducted on the 33-bus distribution test feeders supports that the proposed algorithm achieves stable and satisfactory optimization of STDDs and FTCDs in a model free manner and outperforms existing two-timescale VVC.

REFERENCES

- [1] T. Kurbatova and T. Perederii, “Global trends in renewable energy development,” in *2020 IEEE KhPI Week on Advanced Technology (KhPIWeek)*, Oct. 2020, pp. 260–263.
- [2] M. B. Liu, C. A. Canizares, and W. Huang, “Reactive Power and Voltage Control in Distribution Systems With Limited Switching Operations,” *IEEE Transactions on Power Systems*, vol. 24, no. 2, pp. 889–899, May 2009.
- [3] A. Borghetti, “Using mixed integer programming for the volt/var optimization in distribution feeders,” *Electric Power Systems Research*, vol. 98, pp. 39–50, 2013.
- [4] H. J. Liu, W. Shi, and H. Zhu, “Distributed Voltage Control in Distribution Networks: Online and Robust Implementations,” *IEEE Transactions on Smart Grid*, vol. 9, no. 6, pp. 6106–6117, Nov. 2018.
- [5] T. Xu and W. Wu, “Accelerated ADMM-Based Fully Distributed Inverter-Based Volt/Var Control Strategy for Active Distribution Networks,” *IEEE Transactions on Industrial Informatics*, vol. 16, no. 12, pp. 7532–7543, Dec. 2020.

- [6] H. Zhu and H. J. Liu, "Fast Local Voltage Control Under Limited Reactive Power: Optimality and Stability Analysis," *IEEE Transactions on Power Systems*, vol. 31, no. 5, pp. 3794–3803, Sep. 2016.
- [7] H. Liu and W. Wu, "Online Multi-agent Reinforcement Learning for Decentralized Inverter-based Volt-VAR Control," *IEEE Transactions on Smart Grid*, pp. 1–1, 2021.
- [8] D. B. Arnold, M. Negrete-Pincetic, M. D. Sankur, D. M. Auslander, and D. S. Callaway, "Model-Free Optimal Control of VAR Resources in Distribution Systems: An Extremum Seeking Approach," *IEEE Transactions on Power Systems*, vol. 31, no. 5, pp. 3583–3593, Sep. 2016.
- [9] W. Wang, N. Yu, Y. Gao, and J. Shi, "Safe Off-policy Deep Reinforcement Learning Algorithm for Volt-VAR Control in Power Distribution Systems," *IEEE Transactions on Smart Grid*, pp. 1–1, 2019.
- [10] Y. Gao, W. Wang, J. Shi, and N. Yu, "Batch-Constrained Reinforcement Learning for Dynamic Distribution Network Reconfiguration," *IEEE Transactions on Smart Grid*, pp. 1–1, 2020.
- [11] O. Nachum, S. Gu, H. Lee, and S. Levine, "Data-Efficient Hierarchical Reinforcement Learning," *arXiv:1805.08296 [cs, stat]*, Oct. 2018.
- [12] A. Ecoffet, J. Huizinga, J. Lehman, K. O. Stanley, and J. Clune, "First return, then explore," *Nature*, vol. 590, no. 7847, pp. 580–586, Feb. 2021.
- [13] A. Lazaridis, A. Fachantidis, and I. Vlahavas, "Deep Reinforcement Learning: A State-of-the-Art Walkthrough," *Journal of Artificial Intelligence Research*, vol. 69, pp. 1421–1471, Dec. 2020.
- [14] A. C. Şerban and M. D. Lytras, "Artificial Intelligence for Smart Renewable Energy Sector in Europe—Smart Energy Infrastructures for Next Generation Smart Cities," *IEEE Access*, vol. 8, pp. 77 364–77 377, 2020.
- [15] O. Stanojev, O. Kundacina, U. Markovic, E. Vrettos, P. Aristidou, and G. Hug, "A Reinforcement Learning Approach for Fast Frequency Control in Low-Inertia Power Systems," *arXiv:2007.05474 [cs, eess]*, Jul. 2020.
- [16] D. Zhang, H. Zhang, X. Zhang, X. Li, K. Ren, Y. Zhang, and Y. Guo, "Research on AGC Performance During Wind Power Ramping Based on Deep Reinforcement Learning," *IEEE Access*, vol. 8, pp. 107 409–107 418, 2020.
- [17] H. Liu and W. Wu, "Two-stage Deep Reinforcement Learning for Inverter-based Volt-VAR Control in Active Distribution Networks," *IEEE Transactions on Smart Grid*, pp. 1–1, 2020.
- [18] C. Li, C. Jin, and R. Sharma, "Coordination of PV Smart Inverters Using Deep Reinforcement Learning for Grid Voltage Regulation," in *18th IEEE International Conference on Machine Learning and Applications - ICMLA 2019*, 2019.
- [19] D. Cao, W. Hu, J. Zhao, Q. Huang, Z. Chen, and F. Blaabjerg, "A Multi-Agent Deep Reinforcement Learning Based Voltage Regulation Using Coordinated PV Inverters," *IEEE Transactions on Power Systems*, vol. 35, no. 5, pp. 4120–4123, Sep. 2020.
- [20] Q. Yang, G. Wang, A. Sadeghi, G. B. Giannakis, and J. Sun, "Two-Timescale Voltage Control in Distribution Grids Using Deep Reinforcement Learning," *IEEE Transactions on Smart Grid*, vol. 11, no. 3, pp. 2313–2323, May 2020.
- [21] X. Chen, G. Qu, Y. Tang, S. Low, and N. Li, "Reinforcement Learning for Decision-Making and Control in Power Systems: Tutorial, Review, and Vision," p. 16, 2021.
- [22] W. Zheng, W. Wu, B. Zhang, and Y. Wang, "Robust reactive power optimisation and voltage control method for active distribution networks via dual time-scale coordination," *IET Generation, Transmission Distribution*, vol. 11, no. 6, pp. 1461–1471, 2017.
- [23] Y. Xu, Z. Y. Dong, R. Zhang, and D. J. Hill, "Multi-Timescale Coordinated Voltage/Var Control of High Renewable-Penetrated Distribution Systems," *IEEE Transactions on Power Systems*, vol. 32, no. 6, pp. 4398–4408, Nov. 2017.
- [24] D. Jin, H. Chiang, and P. Li, "Two-Timescale Multi-Objective Coordinated Volt/Var Optimization for Active Distribution Networks," *IEEE Transactions on Power Systems*, vol. 34, no. 6, pp. 4418–4428, Nov. 2019.
- [25] R. R. Jha, A. Dubey, C. Liu, and K. P. Schneider, "Bi-Level Volt-VAR Optimization to Coordinate Smart Inverters With Voltage Control Devices," *IEEE Transactions on Power Systems*, vol. 34, no. 3, pp. 1801–1813, May 2019.
- [26] R. Zafar, J. Ravishankar, J. E. Fletcher, and H. R. Pota, "Multi-Timescale Voltage Stability-Constrained Volt/VAR Optimization With Battery Storage System in Distribution Grids," *IEEE Transactions on Sustainable Energy*, vol. 11, no. 2, pp. 868–878, Apr. 2020.
- [27] R. Lowe, Y. Wu, A. Tamar, J. Harb, P. Abbeel, and I. Mordatch, "Multi-Agent Actor-Critic for Mixed Cooperative-Competitive Environments," *arXiv:1706.02275 [cs]*, Mar. 2020.
- [28] S. Gu, T. Lillicrap, Z. Ghahramani, R. E. Turner, and S. Levine, "Q-Prop: Sample-Efficient Policy Gradient with An Off-Policy Critic," *arXiv:1611.02247 [cs]*, Feb. 2017.
- [29] R. S. Sutton, D. Precup, and S. Singh, "Between MDPs and semi-MDPs: A framework for temporal abstraction in reinforcement learning," *Artificial Intelligence*, vol. 112, no. 1, pp. 181–211, Aug. 1999.
- [30] T. Haarnoja, A. Zhou, K. Hartikainen, G. Tucker, S. Ha, J. Tan, V. Kumar, H. Zhu, A. Gupta, P. Abbeel *et al.*, "Soft actor-critic algorithms and applications," *arXiv preprint arXiv:1812.05905*, 2018.
- [31] P. Sunehag, G. Lever, A. Gruslys, W. M. Czarnecki, V. Zambaldi, M. Jaderberg, M. Lanctot, N. Sonnerat, J. Z. Leibo, K. Tuyls, and T. Graepel, "Value-Decomposition Networks For Cooperative Multi-Agent Learning," *arXiv:1706.05296 [cs]*, Jun. 2017.
- [32] Z. Wang, T. Schaul, M. Hessel, H. van Hasselt, M. Lanctot, and N. de Freitas, "Dueling Network Architectures for Deep Reinforcement Learning," *arXiv:1511.06581 [cs]*, Apr. 2016.
- [33] V. Mnih, A. P. Badia, M. Mirza, A. Graves, T. P. Lillicrap, T. Harley, D. Silver, and K. Kavukcuoglu, *Asynchronous Methods for Deep Reinforcement Learning*, 2016.
- [34] J. Schulman, F. Wolski, P. Dhariwal, A. Radford, and O. Klimov, "Proximal Policy Optimization Algorithms," *arXiv:1707.06347 [cs]*, Aug. 2017.
- [35] G. Brockman, V. Cheung, L. Pettersson, J. Schneider, J. Schulman, J. Tang, and W. Zaremba, *OpenAI Gym*, 2016.
- [36] M. E. Baran and F. F. Wu, "Network reconfiguration in distribution systems for loss reduction and load balancing," *IEEE Transactions on Power Delivery*, vol. 4, no. 2, pp. 1401–1407, 1989.
- [37] J. A. E. Andersson, J. Gillis, G. Horn, J. B. Rawlings, and M. Diehl, "CasADi – A software framework for nonlinear optimization and optimal control," *Mathematical Programming Computation*, vol. 11, no. 1, pp. 1–36, 2019.